RESEARCH ARTICLE

A Lightweight Convolutional Neural Network for Classification of Brain Tumors Using Magnetic Resonance Imaging

Alper Özatılgan[1]* , Mahir Kaya[1]

[1] Tokat Gaziosmanpasa University, Tokat, Türkiye

Corresponding author:
Alper Özatılgan, Tokat Gaziosmanpasa University, Tokat, Türkiye,
ozatilgan_alper@hotmail.com

ABSTRACT

The brain, which controls important vital functions such as vision, hearing and movement, negatively affects our lives when it is sick. Of these diseases, the deadliest is undoubtedly the brain tumor, which can occur in all age groups and can be benign or malignant. Therefore, early diagnosis and prognosis are very important. Magnetic Resonance (MR) images are used for the detection and treatment of brain tumor types. Successful results in the detection of diseases from medical images with Convolutional Neural Networks (CNN) depend on the optimum creation of the number of layers and other hyper-parameters. In this study, we propose a CNN model that will achieve the highest accuracy with the least number of layers. A public data set consisting of 4 different classes (Meningioma, Glioma, Pituitary and Normal) obtained for use in the training of CNN models was trained and tested with 50 different deep learning models designed, and a better result was obtained when compared with the existing studies in the literature with 99.47% accuracy and 99.44% F1 score values.

Keywords: Lightweight model, Brain tumor classification, Convolutional neural network, Deep learning

1. Introduction

The brain is an important organ that controls functions such as thinking, reasoning, speaking, vision, hearing, and the vital functions of the body through the central nervous system, primarily the Cerebrum, which constitutes a large part of the brain [1]. The cerebellum is an organ connected to the brainstem and meninges, supported by nerve cells connected to the brain, spinal cord, and tissues. It is located at the back of the brain, beneath the cerebrum. It is responsible for the body's balance and coordination. Messages necessary for functions controlled by the brain and cerebellum are transmitted by the brainstem. The meninges, known as the brain membrane, are the layers of membranes that surround the central nervous system, including the brain and spinal cord. They protect the brain and spinal cord [2]. The brain, which is of crucial importance for sustaining vital activities, significantly affects our lives when disease occurs [3]. Among these diseases, there is a brain tumor, which threatens all age groups and can be either benign or malignant [1].

A brain tumor is the abnormal growth of cells in the brain. Symptoms of the disease include headaches, unexplained nausea, speech and hearing difficulties, and loss of body control [4]. Unlike other types of cancer, brain tumors and their types are classified not progressively but according to the grades defined by the World Health Organization (WHO), ranging from I to IV, indicating whether they are benign or malignant. Those classified as grades I-II are considered benign, while grades III-IV are considered malignant [5].

Meningioma, which is a type of brain tumor under research, is the most commonly seen type of brain tumor [6]. The World Health Organization (WHO) has identified the most common type as Grade 1 (benign), and the lethal type that occurs intracranially as Grade 3 (malignant) [7]. Atypical meningiomas are classified as Grade II, and this type is more commonly observed in males. Meningiomas more frequently seen in females can be diagnosed using brain imaging techniques for neurological symptoms such as neurological disorders, epilepsy, increased intracranial pressure, as well as nonspecific symptoms like tinnitus and headaches [8].

The most prevalent kind of tumor in the brain and spinal cord are gliomas. They are named based on their histological similarity to healthy glial cells. It is unknown if gliomas originate from neural or glial progenitors, stem cells, or other cell types[9]. Gliomas are among the most common brain tumors, similar to meningiomas, and encompass types such as astrocytoma, oligodendroglioma, glioblastoma, and ependymoma. Classified between grades III-IV by the WHO, gliomas

are categorized as malignant. They are more frequently observed in males compared to females and diagnosed using histopathology [10].

The hypothalamus, located in the lower part of the brain, is where the pituitary gland develops. It produces hormones that regulate essential bodily functions and hormonal systems, thereby controlling various vital functions. Tumors developing in this area can disrupt hormone production, leading to excess or deficiency of certain hormones critical for controlling vital functions [11]. Although classified as benign because it tends not to spread, this type of tumor, known as a pituitary tumor, can impact essential bodily functions and hormonal systems due to its proximity to the brain. Therefore, leaving the mass there can be problematic despite its benign nature [12].

Brain tumors are diagnosed, graded, treated, and tracked using methods including Computed Tomography (CT), Magnetic Resonance Imaging (MRI), and Magnetic Resonance Spectroscopy (MRS). Because it can create high-contrast images even in soft tissues, magnetic resonance imaging (MRI) is the preferred method among these [13]. Using MRI scans and a lightweight CNN model, this study attempts to identify and categorize the types of brain tumors that are pituitary, glioma, and meningioma. Example MRI images related to these types are shown as follows;
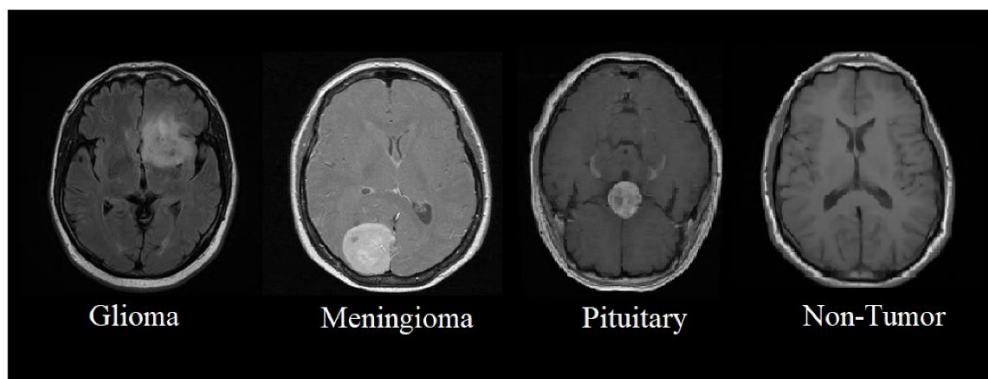

Figure 1. Brain Tumor Types and Normal Image [14]

1.1. Related Works

Detection and classification of brain tumors have been tackled by numerous researchers, who have developed various methods. Many of these methods utilize machine learning and image processing algorithms alongside MRI images.

[15-33] the study conducted research on the classification of brain tumor types (meningioma, glioma, pituitary) in articles. In the study [15], the Back-Propagation Neural Network (BPNN) architecture was used. The proposed architecture was tested on a dataset containing MRI images of three classes, achieving an accuracy of 91.9%. In the study [16], a model derived from Extreme Learning Machines (ELM) algorithm with a CNN structure was used. The proposed model was tested on a dataset containing MRI images of three classes (meningioma, glioma, and pituitary), achieving an accuracy of 93.68%. In the study of Deepak and Ameer [17], transfer learning using GoogleNet was employed for feature extraction from brain MRI images. For classification, SVM and KNN algorithms were applied together with Softmax. The study achieved the highest accuracy rate of 98% with the KNN algorithm. In the study [18], the study proposed a pre-trained CNN model using block-level fine-tuning strategy based on transfer learning. The proposed model was tested on a CE-MRI dataset, achieving an accuracy of 94.82%. In the study[19], they aimed to demonstrate the classification capability of their newly created model on a dataset with two different labels. The proposed model achieved an accuracy rate of 96.13%. In the study of Ghassemi et al. [20], a Generative Adversarial Networks (GAN) based CNN model was proposed for feature extraction from brain MRI images. The proposed model was tested on the dataset, achieving an accuracy of 95.6%. In the study[21], a hybrid model consisting of Neural Autoregressive Distribution Estimation (NADE) and Convolutional Neural Networks (CNN) was used. The proposed model was tested on the dataset, achieving an accuracy of 94.49%. In the study[22], images in the dataset were first processed using Local Binary Pattern (LBP) to extract effective features. Subsequently, classification methods including K-Nearest Neighbor (KNN), Artificial Neural Networks (ANN), Random Forest (RF), and Linear Discriminant Analysis (LDA) were employed. The proposed method was tested on the dataset, achieving an accuracy of 95.56%. In the study of Rehman et al.[23], they used AlexNet, GoogleNet, and VGGNet CNN models. They achieved the highest accuracy of 98.69% with VGGNet. In the study [24], a new CNN model with various layers was proposed to classify brain tumor types. It was observed that the proposed model outperformed other models with an accuracy of 94.74% on three different datasets. In the study [25], two different CNN architectures were used for identification and classification. Testing the proposed CNN architecture on two datasets resulted in an accuracy of 97.3%. In the study of Sowrirajan et al.[26], a newly created CNN model called VGG16-NADE was used and compared with other methods. The proposed model achieved a prediction accuracy of 96.01%. In the study [27], they tested the proposed new deep learning model on two different datasets. The proposed model demonstrated an accuracy rate of 98.57%. In the study [28], a 13-layer CNN architecture was used. The proposed CNN architecture was tested on a dataset consisting of 3064 MRI images from three classes, achieving a highest accuracy of 97.2%.

In the study of Nasiri et al. [29], a fine-tuned (Block-Wise) VGG19 (BW-VGG19) architecture was proposed. The proposed method was tested on the CE-MRI dataset, achieving an accuracy of 98%. In the study of Kaya and Çetin-Kaya [30], the detection of pneumonia disease in lung images obtained via X-ray was aimed. X-ray images from balanced and imbalanced datasets were processed by separating them from noise to extract lung images. These images were organized, and a new CNN architecture, trained and tested with optimal weights determined by Genetic Algorithm (GA), was created. At the end of the study, it was observed that the GA-based ensemble CNN architecture performed optimally on the balanced dataset, achieving the highest accuracy of 97.23%. In the study of Kaya and Çetin-Kaya [31], a simple CNN based on fine-tuned hyperparameters was developed to detect the severity of Alzheimer's disease. The proposed model was trained on publicly available Alzheimer's dataset and achieved an accuracy of 99.53%. In the study of Kaya[32], the study aimed to detect brain tumor types using MRI images. Two separate datasets, Dataset 1 and Dataset 2, were used in this study, with Dataset 1 having fewer images compared to Dataset 2. The proposed model, a 9-layer CNN architecture trained on Dataset 2, demonstrated outstanding performance with an accuracy of 99.62%. In the study of Çetin-Kaya and Kaya [33], different CNN architectures were used along with transfer learning and fine-tuning for detecting brain tumor types from MRI images. Three datasets with different quantities of samples and classes were used to train the models. With an accuracy of 99.92%, the suggested model performed well after being trained on the dataset containing the greatest amount of data.

1.2. Motivation

Finding the best course of treatment and detecting brain tumors early are essential for survival. Radiologists and physicians will have less work to complete when computer systems are used to automate the classification, which would expedite the treatment decision-making process. CNN architecture is commonly used in disease detection studies from computerized graph images. Therefore, in this study, we aim to develop a new CNN architecture with modified parameters and layer numbers to achieve high accuracy.

In previous studies related to brain tumor detection, it has been observed that some CNN architectures are overly complex and achieve lower accuracy values than expected. In this study, we aim to develop a new model with minimal layers and parameters to achieve high accuracy and low error rates, enabling its use across different platforms.

1.3. Contributions

In this study, we started with the minimum number of layers as shown in Table 3. We trained and tested 50 different models with varying numbers of layers and parameter values. Among the 50 different architectures we created, we identified several models with the highest accuracy rates.

At the end of this study, we proposed a lightweight model with minimal parameters and highest accuracy for classifying brain tumor types.

2.   Materials and Methods

2.1. Dataset

In the study, we utilized a Kaggle dataset consisting of four classes: Meningioma, Glioma, Pituitary, and Normal, representing diseased and healthy samples. [34]. This dataset contains 1339 MRI images of Meningioma patients, 1321 MRI images of Glioma patients, 1457 MRI images of Pituitary patients, and 1595 MRI images of Normal (healthy) subjects for training purposes. The validation data was created by taking a %5 percent from the training dataset, while the test set consists of 306 MRI images of Meningioma patients, 300 MRI images of Glioma patients, 300 MRI images of Pituitary patients, and 405 MRI images of Normal (healthy) subjects.

2.2. Convolutional Neural Network

Convolutional Neural Networks (CNNs) are deep learning algorithms that recognize objects in images by using images as input [35]. This algorithm, which captures features in images in different operations, consists of different layers. [31, 36].

Three major components make up CNN: the pooling layer, which is used to classify the network, the fully connected layer, which is used to extract features and is the first layer in deep learning models, and the convolution layer [30,35]. CNNs have layers like normalization, pooling, and dropout and are feedforward artificial neural networks in terms of architecture. [32,37]. To maintain spatial structure, neurons that share the same filter are only connected to local regions of the image; weights are shared to minimize the number of parameters in the model [35].

The general architectural overview of CNN is illustrated in Figure 2 below;
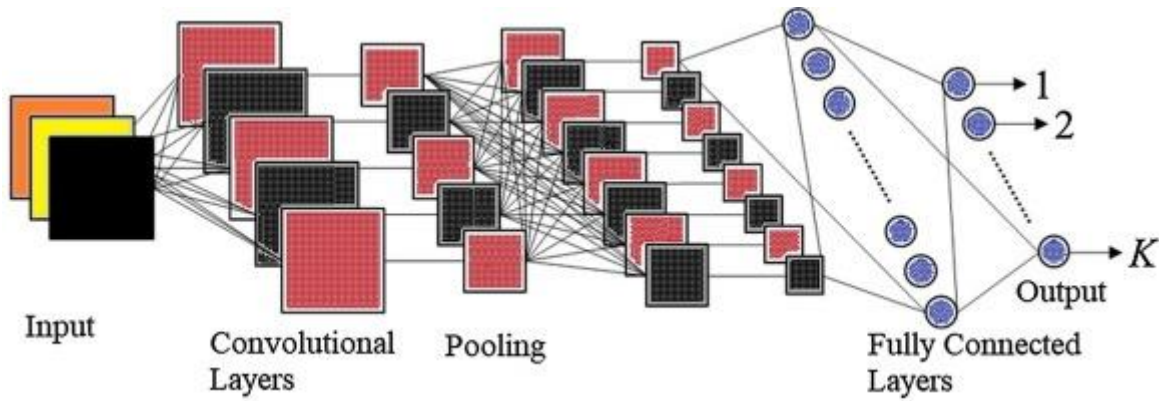
Figure 2. CNN Architecture [38]

2.2.1. CNN Layers

Convolutional Layer

It allows extracting features from input images by using a combination of linear and non-linear operations. This layer generates new images where features are identified from the input image [40]. The mathematical expression of the convolutional layer is shown in Equation 1 [41].

$$S(i,j) = (I * K)(i,j) = \sum\sum I(i + m, j + n)K(m,n) \tag{1}$$

In Equation 1, I, represents the input image, K, represents the kernel, and S denotes the output after the convolution operation.

Activation Function

It is used to introduce complex data such as nonlinear audio, images, video, and text to neural networks. Without using an activation function, there is no possibility of improvement in training neural networks [42]. Training and learning are improved with an activation function, providing better generalization [43]. Sigmoid (Equation 2), ReLU (Equation 3), Leaky ReLU (Equation 4), Softmax (Equation 5), and Tanh (Equation 6) are preferred activation functions [44]. The mathematical expressions of some activation functions are as follows [45];

$$sigmoid(x) = \frac{e^x}{1 + e^x} \tag{2}$$

$$R(x) = \begin{cases} x & if\ x \geq 0 \\ 0 & otherwise \end{cases} \tag{3}$$

$$R(x) = \begin{cases} x & if\ x \geq 0 \\ \infty x & otherwise \end{cases} \tag{4}$$

$$Yi = \frac{e^{z_i}}{\sum_{i=0}^{m} e^{z_i}} \tag{5}$$

$$\tan h(x) = \frac{e^x - e^{-x}}{e^x + e^{-x}} \tag{6}$$

Pooling Layer

The layer that follows convolutional layers in convolutional neural network architecture. The function of this layer is to reduce the dimensions of the image by taking either the average (average pooling) or maximum value (max pooling) of pixels in a specific area of the input image, following the convolutional layer. If this layer is not used, the computational operations would be costly. Although there is pixel loss in this layer, preventing overfitting by reducing computational operations [46]. The pooling layer's job is to integrate semantically related information, whereas the convolutional layer's job is to recognize local combinations of features from earlier layers [49]. General formula of a block can be represented as in Equation 7:

$$MaxPooling\left(Act\left(BN\left(Conv(X_i, K_i)\right)\right)\right) \tag{7}$$

Fully Connected Layer

This layer examines the features of the object revealed from the convolutional and pooling layers, identifies neurons containing weights that specify the object's characteristics, and performs classification of the object [42]. The mathematical expressions of fully connected layer are shown in Equation 8 [48];

$$yi' = \sum_i W_{ii'}X_i + b_{i'} \tag{8}$$

Dropout Layer

Training a multi-layered network requires excessive computation and a large amount of data. This data may not be sufficient to train different networks on different subsets of the data. Dropout is used to address overfitting and insufficient data issues that may arise in created convolutional neural networks. [47].

3. Proposed Model

When considering past similar research activities and especially common methods used in artificial intelligence for image processing in medical images, the goal in our proposed method is to achieve the best results by using convolutional, pooling, and fully connected layers at an optimal minimum number, different from previously known architectures, and to determine which type of brain tumor is present in MRI images.

In our proposed model, we created a CNN model with 6 convolutional layers, different from known architectures. In the final layer, we created an output layer with 4 neurons corresponding to the 4 classes in our dataset. The hyperparameter values of this model are listed in Table 1;

Table 1 Best hyperparameter result

Layer	Filter Size	Kernel Size
Conv. Layer	16	3x3
Conv. Layer	32	3x3
Conv. Layer	64	3x3
Conv. Layer	128	3x3
Conv. Layer	256	3x3
Conv. Layer	512	3x3
Dense Layer	128	-

The proposed CNN architecture of our model, which consists of 6 convolutional layers with filter counts of 16, 32, 64, 128, 256, and 512 respectively, along with a Dense layer that has a number of filters equal to the number of classes (128), is shown in Figure 3 below;
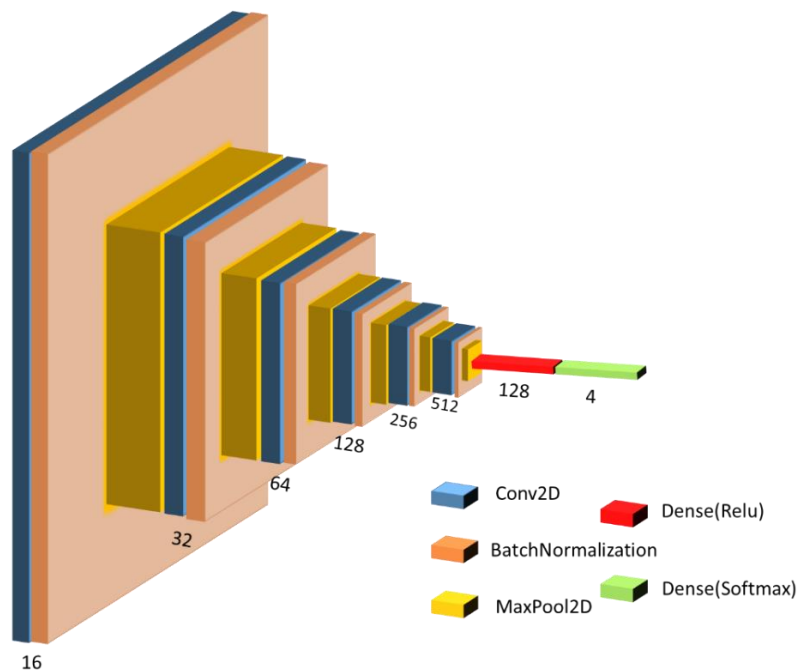

Figure 3. Proposed CNN Model Architecture

Evaluation of Performance

The detection performance of our proposed model is evaluated by important statistical measures such as recall, precision and accuracy. These measures are summarized as follows;

TP: Number of correct guesses from positive situations

TN: Number of correct guesses from negative situations.

FP: Number of incorrect guesses from positive situations

FN: Number of incorrect guesses from negative situations.

Accuracy

It is a metric that assesses how well a method performs by calculating the proportion of accurate forecasts to all predictions. Mathematically, it is expressed in Equation 9;

$$Accuracy = \frac{TP + TN}{TP + FP + TN + FN} \tag{9}$$

Precision

It displays the proportion of positively projected classes that are actually positive. Mathematically, it is expressed in Equation 10;

$$Precision = \frac{TP}{TP + FP} \tag{10}$$

Recall

It shows how many positive samples in the image were correctly predicted. Mathematically, it is expressed in Equation 11;

$$Recall = \frac{TP}{TP + FN} \tag{11}$$

Specificity

The rate of correctly predicted negative states to all actual negative states. Mathematically, it is expressed in Equation 12;

$$Specificity = \frac{TN}{FP + TN} \tag{12}$$

F1-Score

A measurement that combines recall and precision by averaging harmonics. It balances Precision and Recall[35]. Mathematically, it is expressed in Equation 13;

$$f1 - Score = 2x \frac{Precision \; x \; Recall}{Precision + Recall} \tag{13}$$

4. Experimental Results

In the study, training was conducted on a system equipped with an i7 3.0 GHz processor, 16 GB RAM, and an Nvidia GeForce GTX 1060 graphics card. Our proposed model is a 6-layer convolutional model trained on the 'Training' folder of the dataset, split into 95% for training and 5% for validation. The images in our dataset were resized to 224x224x3 dimensions and trained and tested by different models created by modifying hyperparameters as specified in Table 3, along with our proposed model. The Confusion Matrix values obtained for our model with the highest accuracy rate achieved at the testing dataset for each class in Figure 4;
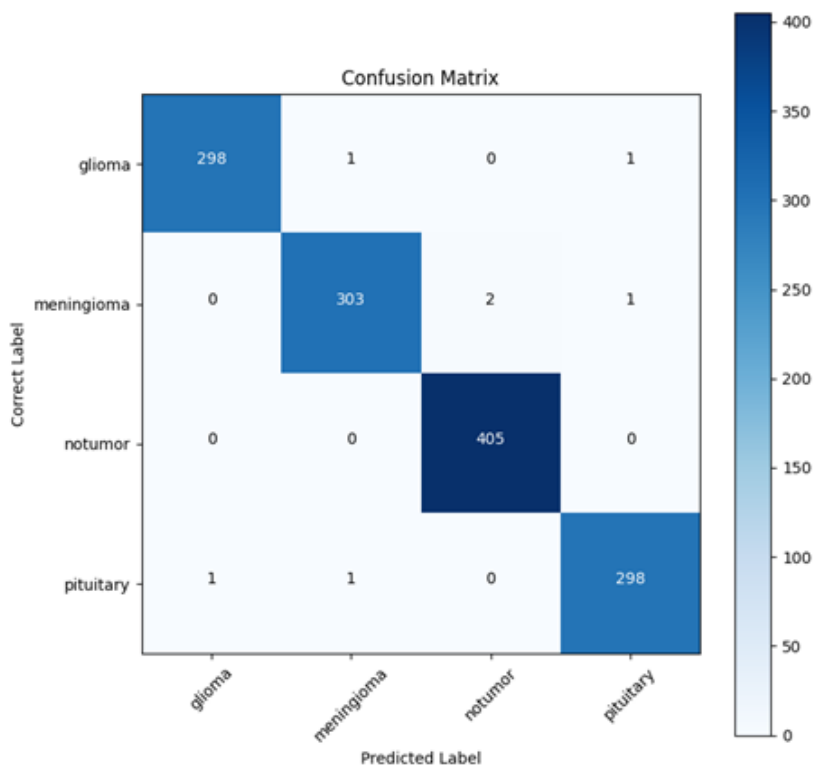
Figure 4. Confusion Matrix Table of the Proposed Model

The precision, recall, and f1-score values of our proposed model suggested from this table are shown in Table 2;

Table 2. Values of Proposed Model

Model	Precision	Recall	F1-Score
Proposed Model	0,99462	0,99421	0,99442

The accuracy and loss curves formed by the accuracy and loss values obtained at each training and testing step of the proposed model are shown in Figure 5;
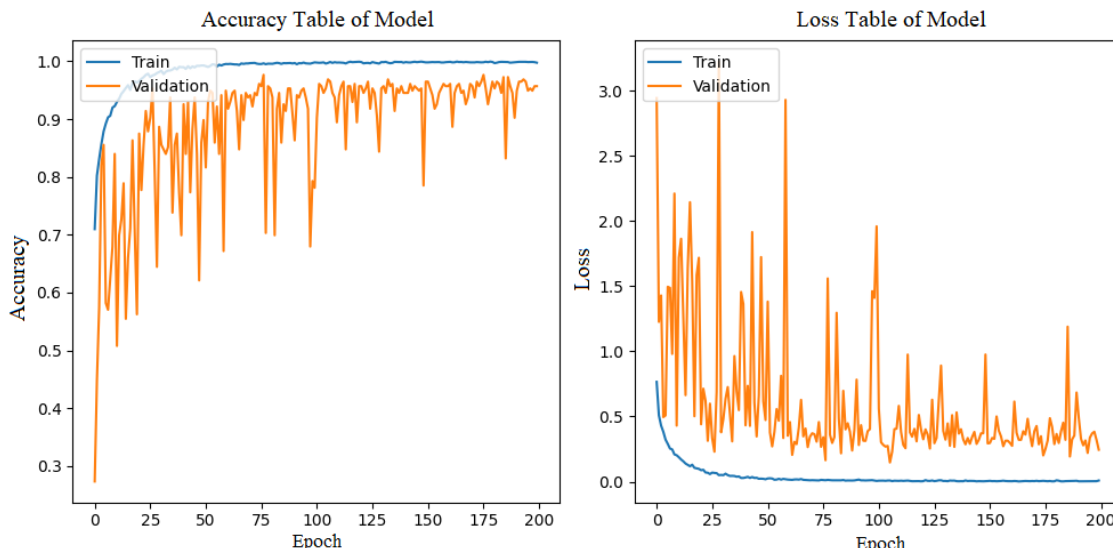
Figure 5. Accuracy and Loss Graph of Proposed Model

In Table 3, we trained 50 different CNN models by the dataset used for diseases from brain MRI images, along with the numbers of convolutional and dense layers, batch size, optimization method, kernel size, and the ratio of training and validation images from the 'Training' folder in the dataset, aiming to find our best-performing model. The accuracy, precision, and f1-score values obtained from training these models are summarized in the table below. Each row in Table 3 represents a proposed model architecture that has been trained and tested.

Table 3. Created Different CNN Models and Their Results (*:ADAM, **:SGD)

Con_1	Kernel_size	Con_2	Kernel_size	Con_3	Kernel_size	Con_4	Kernel_size	Con_5	Kernel_size	Con_6	Kernel_size	Con_7	Kernel_Size	Dense	Batch_size	Optimization	Epoch	Accuracy(%)	Precision(%)	F1-Score(%)
16	3	32	3	64	3	128	3							64	16	*	100	98.70	98.70	98.65
16	3	32	3	64	3	128	5							64	32	**	100	87.80	90.48	86.13
16	3	32	3	64	3	128	5							128	32	**	100	98.47	98.41	98.40
16	3	32	3	64	3	128	3	256	3					64	16	*	100	99.39	99.36	99.36
16	3	32	3	64	3	128	3	256	3					128	16	**	100	98.63	98.57	98.55
16	3	32	3	64	3	128	3	256	3					128	16	**	100	98.25	98.21	98.14
16	3	32	3	64	3	128	3	256	3					128-64	16	**	100	97.10	97.08	96.89
16	3	32	3	64	3	128	3	256	3					64	16	**	100	97.48	97.49	97.37
16	3	32	3	64	3	128	3	256	3					64	16	**	150	96.87	96.89	96.63
16	3	32	3	64	3	128	3	256	3					64	32	**	150	99.39	99.34	99.35
16	3	32	3	64	3	128	3	256	3					64	64	**	100	98.86	98.85	98.81
16	3	32	3	64	3	128	3	256	3	256	3			64	16	*	100	97.64	97.60	97.45
16	3	32	3	64	3	128	3	256	3	256	3			64	16	**	100	97.79	97.74	97.62
32	3	64	3	128	3	256	3							64	16	*	100	97.33	97.37	97.18
32	3	64	3	128	3	256	3	512	3					64	16	*	100	98.02	97.97	97.87
64	3	128	3	256	3	512	3							64	16	*	100	93.52	93.73	93.20
16	3	32	3	64	3	128	3	256	3	512	3			64	16	**	100	98.86	98.83	98.79
16	3	32	3	64	3	128	3	256	3	512	3			128	32	**	100	99.31	99.30	99.28
16	5	32	3	64	3	128	3	256	3	512	3			128	32	**	100	98.32	98.31	98.20
16	5	32	5	64	5	128	5	256	5	512	5			128	32	**	100	97.25	97.32	97.06
16	3	32	3	64	3	128	3	256	3	512	5			128	32	**	100	99.16	99.18	99.13
16	3	32	3	64	3	128	3	256	3	512	5			128	32	**	130	99.01	98.99	98.97
16	3	32	3	64	3	128	3	256	3	512	5			128	32	**	150	99.01	99.03	98.98
16	3	32	3	64	3	128	3	256	3	512	5			128	32	**	180	99.39	99.42	99.38
16	3	32	3	64	3	128	3	256	3	512	5			128	32	**	200	98.47	98.46	98.38
16	3	32	3	64	3	128	3	256	5	512	5			128	32	**	100	97.56	97.54	97.37
16	5	32	3	64	3	128	3	256	3	512	3			128	32	**	150	83.07	87.92	80.00
16	3	32	5	64	5	128	3	256	3	512	5			128	32	**	100	98.86	98.80	98.79
16	3	32	5	64	5	128	3	256	3	512	5			128	16	**	100	99.24	99.22	99.19
16	3	32	5	64	5	128	3	256	3	512	5			128	16	**	100	99.39	99.38	99.36
16	3	32	5	64	5	128	3	256	3	512	5			128	16	**	100	98.78	98.72	98.71
16	3	32	5	64	5	128	3	256	3	512	5			128	16	*	100	98.70	98.66	98.61
16	3	32	5	64	5	128	3	256	3	512	5			128	16	**	125	99.39	99.38	99.36
16	3	32	3	64	3	128	3	256	3	512	3			128	32	*	100	97.71	97.72	97.59
16	3	32	3	64	3	128	3	256	3	512	3			128	32	**	100	99.24	99.26	99.21
16	3	32	3	64	3	128	3	256	3	512	3			256	32	**	100	98.63	98.58	98.55
16	3	32	3	64	3	128	3	256	3	512	3			256	16	**	100	94.51	95.08	94.07
16	3	32	3	64	3	128	3	256	3	512	3			512	32	*	100	95.19	95.35	94.87
16	3	32	3	64	3	128	3	256	3	512	3			128	32	**	100	99.24	99.26	99.21
16	3	32	3	64	3	128	3	256	3	512	3			128	32	**	130	99.39	99.39	99.36
16	3	32	3	64	3	128	3	256	3	512	3			128	32	**	150	99.31	99.32	99.28
16	3	32	3	64	3	128	3	256	3	512	3			128	32	**	170	97.86	97.84	97.71
16	**3**	**32**	**3**	**64**	**3**	**128**	**3**	**256**	**3**	**512**	**3**			**128**	**32**	****	**200**	**99.47**	**99.46**	**99.44**
16	5	32	3	64	3	128	3	256	3	512	3			128	32	**	100	98.32	98.31	98.20
16	5	32	3	64	3	128	3	256	3	512	3			128	32	**	150	83.07	98.92	80.00
16	5	32	3	64	3	128	3	256	3	512	3			128	32	**	100	98.32	98.31	98.20
16	5	32	3	64	3	128	3	256	3	512	3			128	32	**	150	83.07	98.92	80.00
16	3	32	5	64	3	128	5	256	3	512	5	1024	3	128	16	**	100	99.24	99.21	99.19
16	3	32	3	64	3	128	3	256	3	512	3	1024	3	512	32	**	100	87.26	90.65	86.21
16	3	32	3	64	3	128	3	256	3	512	3	1024	3	256	16	*	100	98.63	98.54	98.54

4.1. Comparison of the Proposed Model with Studies in Literature

Table 4 displays a comparison of our suggested model's accuracy, precision, and f1-score values with those from earlier research.

Table 4. Comparison of Our Model with Previous Studies

Author	Model	Performance Measures		
		Accuracy	**Precision**	**F1-Score**
Kaplan et al.	nLBP+KNN	0,9556	0,956	0,956
Ghassemi et al.	Random Division and GAN method	0,956	0,9529	0,9510
Sowrirajan et al.	Hybrid VGG16-NADE	0,9601	0,9572	0,9568
Sultan et al.	Not specified	0,9613	0,9342	0,9475
Kibriya et al.	CNN Architecture with 13 Layers	0,972	0,97	0,9709
Haq et al.	GoogleNet Variable Architecture	0,973	0,9374	0,9548
Deepak et al.	GoogleNet+SVM	0,98	0,97	0,9749
Asiri et al.	BW-VGG19	0,98	0,9843	0,9821
Yerukalareddy et al.	CNN with GAN	0,9857	0,9875	0,9865
Rehman et al.	VGG16 with Fine Tuned	0,9869	-	-
Proposed Model	**6 Conv. Layer CNN**	**0,9947**	**0,99462**	**0,99442**

4.2. Comparison of the Proposed Model with Transfer Learning Models

In this study, well-known transfer learning models such as VGG16, DenseNet121, InceptionV3, ResNet50, MobileNetV2, and EfficientNetB0 were trained on the dataset, provided that the epoch, batch size, and optimization values applied in our proposed model remained the same. The results obtained from this training and the total parameter values are presented in Table 5.

Tablo 5. Comparison of Our Model with Transfer Learning Models

Model	Opt.	Batch-Size	Epoch	Accuracy (%)	Total Params
InceptionV3	SGD	32	200	92.98	22 million
MobileNetV2	SGD	32	200	94,96	3.4 million
DenseNet121	SGD	32	200	95.72	7.2 million
VGG16	SGD	32	200	96.87	14.8 million
ResNet-50	SGD	32	200	97.02	23.9 million
EfficientNetB0	SGD	32	200	99.46	4.2 million
Proposed Model	**SGD**	**32**	**200**	**99.47**	**2.2 million**

When Table 5 is examined, the accuracy values of the EfficientNetB0 model and the model we proposed gave almost the same accuracy result. Since EfficientNet model types dynamically increase the depth and width (compound scaling), they generally gives successful results in the medical image classification. However, our proposed architecture has approximately half as many parameters as the EfficientNetB0 model. Thus, our proposed architecture outperforms existing transfer learning models.

5. Discussion

This study developed a new CNN model with 6 convolutional layers for automatically detecting brain tumor types (Meningioma, Glioma, Pituitary) using brain MRI images. The dataset used consists of a total of 4 classes: 3 different diseased conditions and 1 normal class, sourced from the Kaggle database. According to results obtained from previous studies in the literature, our proposed model has shown superior performance.

When examining the CNN models created with different hyperparameter values in Table 3, it was observed that the SGD optimization algorithm outperformed the ADAM algorithm in terms of performance. Setting a high kernel value in the first layer adversely affected its performance; however, improvement was observed in performance when higher kernel values were used in subsequent layers. It was observed that the optimal value for the Dense layer is 128 based on the activation functions of preceding layers, and it was determined that the ADAM optimization algorithm produces better results with lower values. In some models, the accuracy values tended to decrease with increasing epochs initially, but it was observed that they started to rise again afterward.

Figure 5 displays the training and validation accuracy plot of the proposed model. When looking at this graph, it can be observed that at certain epoch values, the training and validation curves converge and overlap, while at specific epoch values, the gap between them widens. According to this graph, it is evident that the model exhibits a little sign of overfitting during the training phase. Figure 5 shows the training and validation loss plot of the proposed model. When looking at the loss plot, it is observed that although the difference between training and validation accuracy curves has increased at some epoch values, both accuracy and loss values for 'train' and 'validation' have moved closely together in both graphs.

In Table 4, when comparing our proposed model with previous studies, feature extraction processes were applied before implementing the deep learning model on the dataset in studies [17] and [22]. The model underwent pre-training and was subsequently retrained on the classification model in the study [20]. Despite other studies using more layers than our proposed model, our model achieved higher accuracy than previous studies.

According to Table 5, our model achieved the highest accuracy among the used transfer learning models with the least number of parameters.

6. Conclusion

By using computer technologies to detect brain tumors automatically and reliably at an early stage, physicians' workloads will be reduced and errors coming from manual examination would be eliminated. In order to detect diseases from medical photos, CNN models are frequently utilized. We optimized the hyperparameters in the CNN architecture to achieve the highest accuracy with a CNN model with the fewest parameters for the brain tumor dataset.

As seen in Table 3, 50 different models have been developed in accordance with the objectives of our study. Among these developed models, we have achieved the highest accuracy of 99.47% with the fewest number of layers and minimal hyperparameters. In the future, other hyperparameter selection techniques that determine the model's performance can be developed and tested using different CNN models, and by increasing the number of data in the dataset, better results can be achieved with new techniques.

References

[1]   R. Singh, C. Prabha, S. Kumari, K. Murugan, M. R. Veeramanickam and T. Singh, "Accuracy Enhancement in Detecting Pituitary Tumors Using Deep Learning," *In 2023 International Conference on Sustainable Communication Networks and Application (ICSCNA)*, pp:1067-1072, IEEE, 2023

[2]   L. Thau, V. Reddy, and P. Singh, "Anatomy, central nervous system," In StatPearls [Internet]. StatPearls Publishing, 2022

[3]   B-L. Isabelle *et al*, "The Global Brain Health Survey: Development of a Multi-Language Survey of Public Views on Brain Health," *Front. Public Health, Sec. Public Health Education and Promotion*, Vol:8, doi: https://doi.org/10.3389/fpubh.2020.00387, 2020

[4]   J. Cahill, G. LoBiondo-Wood, N. Bergstrom, and T. Armstrong, "Brain tumor symptoms as antecedents to uncertainty: An integrative review," *Journal of Nursing Scholarship*, vol. 44, no. 2, pp:145-155, 2012

[5]   J. S. Barnholtz-Sloan, Q. T. Ostrom, D. Cote, "Epidemiology of Brain Tumors," *Neurologic Clinics*, Vol. 36, Issue 3, pp:395-419, 2018

[6]   A-R. Fathi and U. Roelcke, "Meningioma," *Neuro-Oncology (Le Abrey, Section Editor) Curr Neurol Neurosci*, Vol. 13, no.337, Doi:10.1007/s11910-013-0337-4, 2013

[7]   J. Wiemels, M. Wrensch and E. B. Claus, "Epidemiology and Etiology of Meningioma," *Invited Review, J*

Neurooncol, Vol. 99, pp:307-314, Doi: 10.1007/s11060-010-0386-3, 2010

[8]   C. Apra, M. Peyre and M. Kalamarides, "Current Treatment Options for Meningioma," *Expert Review of Neurotherapeutics, HAL Open Science*, Vol. 18, no. 3, pp:241-249, 2018

[9]   A.S. Modrek, N.S. Bayin and D.G. Placantonakis, "Brain Stem Cells as the Cell of Origin in Glioma," *World J Stem Cells*, Vol. 6, no. 1, pp:43-52, 2014

[10]   N. A. O. Bush, S. M. Chang and M. S. Berger, "Current and Future Strategies for Treatment of Glioma," *Neurosurg Rev*, vol. 40, pp:1-14, 2017

[11]   S. D. Muhammad and Z. Kobti, "An Ensemble Deep Learning Approach for Enhanced Classification of Pituitary Tumors," *In 2023 IEEE Symposium Series on Computational Intelligence, IEEE*, p: 427-432, 2023

[12]   A. M. Gab Allah, A. M. Sarhan and N. M. Elshennawy, "Classification of brain MRI tumor images based on deep learning PGGAN Augmentation," *Diagnostics*, Vol. 11, no. 12, 2021

[13]   M. K. Abd-Ellah, A. I. Awad, A. A. Khalaf and H. F. Hamed, "A review on brain tumor diagnosis from MRI images: Practical implications, key achievements, and lessons learned," *Magnetic resonance imaging*, Vol. 61, pp: 300-318, 2019

[14]   S. A. Yazdan, R. Ahmad, N. Iqbal, A. Rizwan, A. N. Khan, and D. H. Kim, "An efficient multi-scale convolutional neural network based multi-class brain MRI classification for SaMD," *Tomography*, Vol. 8, no. 4, pp:1905-1927, 2022

[15]   M. R. Ismael and I. Abdel-Qader, "Brain Tumor Classification via Statistical Features and Back-Propagation Neural Network," *2018 IEEE Uluslararası Elektro/Bilgi Teknolojisi Konferansı*, 2018.

[16]   A. Pashaei, H. Sajedi and N. Jazayeri, "Brain Tumor Classification via Convolutional Neural Network and Extreme Learning Machines," *ICCKE2018, Ferdowsi University of Mashhad*, pp: 314-319

[17]   S. Deepak, P.M. Ameer, "Brain tumor classification using deep CNN features via transfer learning," *Computers in Biology and Medicine, ELSEVIER*, 2019

[18]   Z. N. K. Swati, Q. Zhao, M. Kabir, F. Ali, S. Ahmed and J. Lu, "Brain Tumor Classification for MR Images Using Transfer Learning and Fine-Tuning," *Computerized Medical Imaging and Graphics, ELSEVIER*, 2019

[19]   H. H. Sultan, N. M. Salem and W. Al-Atabany, "Multi-classification of brain tumor images using deep neural network," *IEEE Access*, Vol. 7, pp:69215–69225, 2019

[20]   N. Ghassemi, A. Shoeibi and M. Rouhani, "Deep neural network with generative adversarial networks pre-training for brain tumor classification based on MR images," *Biomedical Signal Processing and Control, Elsevier*, 2020 doi: https://doi.org/10.1016/j.bspc.2019.101678

[21]   R. Hashemzehi, S. J. S. Mahdavi, M. Kheirabadi and S. R. Kamel, "Detection of brain tumors from MRI images base on deep learning using hybrid model CNN and NADE," *Biocybernetics And Biomedical Engineering, Elsevier*, pp: 1225-1232, doi: https://doi.org/10.1016/j.bbe.2020.06.001, 2020

[22]   K. Kaplan, Y. Kaya, M. Kuncan and H. M. Ertunç, "Brain tumor classification using modified local binary patterns (LBP) feature extraction methods," *Medical Hypotheses, Elsevier*, doi: https://doi.org/10.1016/j.mehy.2020.109696 , 2020

[23]   A. Rehman, S. Naz, M. I. Razzak, F. Akram, and M. Imran, "A deep learning based framework for automatic brain tumors classification using transfer learning," *Circuits, Systems, and Signal Processing*, Vol. 39, no. 2, pp:757–775, doi:10.1007/S00034-019-01246-3/TABLES/8, 2020

[24]   W. Ayadi, W. Elhamzi, I. Charfi and M. Atrl, "Deep CNN for Brain Tumor Classification," *Neural Processing Letters, Springer*, Vol. 53, pp:671-700, doi: https://doi.org/10.1007/s11063-020-10398-2 , 2021

[25]   E. U. Haq, H. Jianjun, K. Li, H. U. Haq and T. Zhang, "An MRI-based deep learning approach for efficient classification of brain tumors," *Journal of Ambient Intelligence and Humanized Computing, Springer*, doi: https://doi.org/10.1007/s12652-021-03535-9 , 2023

[26]   S. R. Sowrirajan, S. Balasubramanian and R. S. P. Raj, "MRI Brain Tumor Classification Using a Hybrid VGG16-NADE Model," *Article-Engineering, Technology and Techniques, BABT*, Vol. 66 doi: https://doi.org/10.1590/1678-4324-2023220071 ,2022

[27]   D. R. Yerukalareddy and E. Pavlovskiy, "Brain Tumor Classification Based on MR Images Using Gan as a Pre-trained Model," *IEEE Ural-Siberian Conference On Computational Technologies in Cognitive Science, Genomics And Biomedicine (CSGB)*, pp:380-384, doi: 10.1109/CSGB53040.2021.9496036, 2021

[28]   H. Kibriya, M. Masood, M. Nawaz, T. Nazir, "Multiclass classification of brain tumors using a novel CNN architecture," *Multimedia Tools and Applications, SPRINGER,* Vol. 81, pp:29847-29863, doi: https://doi.org/10.1007/s11042-022-12977-y ,2022

[29]   A. A. Nasiri et al, "Block-Wise Neural Network for Brain Tumor Identification in Magnetic Resonance Images," *Computers, Materials & Continua, Tech Science Press*, Vol. 73, no.3, pp: 5735-5753, doi: 10.32604/cmc.2022.03174, 2022

[30]   M. Kaya, and Y. Çetin-Kaya, "A novel ensemble learning framework based on a genetic algorithm for the classification of pneumonia," *Engineering Applications of Artificial Intelligence*, Vol. 133, no. 108494, 2024

[31]   M. Kaya and Y. Çetin-Kaya, "A Novel Deep Learning Architecture Optimization for Multiclass Classification of Alzheimer's Disease Level," *IEEE Access*, 2024

[32]   M. Kaya, "Bayesian Optimization-based CNN Framework for Automated Detection of Brain Tumors," *Balkan Journal of Electrical and Computer Engineering*, Vol. 11, no. 4, pp:395-404, 2023

[33]   Y. Çetin-Kaya and M. Kaya, "A Novel Ensemble Framework for Multi-Classification of Brain Tumors Using Magnetic Resonance Imaging," *Diagnostics*, Vol. 14, no. 4, 2024

[34]   https://www.kaggle.com/datasets/masoudnickparvar/brain-tumor-mri-dataset

[35]   K. O'Shea and R. Nash, "An Introduction to Convolutional Neural Networks," *arXiv:* 1511.08458v2, 2015

[36]   E. Cengil and A. Çınar, "A New Approach For Image Classification: Convolutional Neural Network," *Europan Journal of Technic, INESEG*, Vol 6, Num 2, pp: 96-103, 2016

[37]   E. Ö. YILMAZ and T. KAVZOĞLU, "Derin Öğrenmenin Temel Prensipleri ve Uzaktan Algılama Alanındaki Uygulamaları," *Harita Dergisi*, Vol. 166, pp. 25-43, 2021

[38]   F. Özyurt, E. Sert, E. Avci, and E. Dogantekin, "Brain tumor detection based on Convolutional Neural Network with neutrosophic expert maximum fuzzy sure entropy," *Measurement*, Vol. *147*, no. 106830, 2019

[39]   Y. Lu, S. Yi, N. Zeng, Y. Liu and Y. Zhang, "Identification of rice diseases using deep convolutional neural networks," *Neurocomputing*, *Elsevier*, Vol. 267, pp:378-384, 2017

[40]   R. Yamashita, M. Nishio, R. K. G. Do and K. Togashi, "Convolutional Neural Networks: An Overview and Application in Radiology," *Insights Into Imaging,* Vol. 9, no. 4, pp:611-629, 2018

[41]   I. Goodfellow, Y. Bengio, A. Courville, "Deep learning," *MIT Press*, 2016

[42]   W. Hao, W. Yizhou, L. Yaqin and S. Zhili, "The Role of Activation Function in CNN," *Proceedings, 2020 2nd International Conference on Information Technology and Computer Application*, *ITCA*, pp:429-432, doi: https://doi.org/10.1109/ITCA52113.2020.00096, 2020

[43]   B. Singh, S. Patel, A. Vijavvargiya and R. Kumar, "Analyzing the Impact of Activation Functions on the Performance of the Data-Driven Gait Model," *Results in Engineering*, Vol. 18, 2023

[44]   S. Sharma, S. Sharma and A. Athaiya, "Activation Functions in Neural Networks," *International Journal of Engineering Applied Sciences and Technology*, Vol. 4 no. 12, pp:310-316, 2020

[45]   S. R. Dubey, S. K. Singh and B. B. Chaudhuri, "Activation functions in deep learning: A comprehensive survey and benchmark," *Neurocomputing*, Vol. 503, 92-108, 2022

[46]   Bayram F., "Derin Öğrenme Tabanlı Otomatik Plaka Tanıma," *Politeknik Dergisi*, Vol. 23, no. 4, pp:955-960, 2020

[47]   N. Srivastava, G. Hinton, A. Krizhevsky, I. Sutskever, R. Salakhutdinov, "Dropout: A Simple Way to Prevent Neural Networks from Overfitting," *Journal of Machine Learning Research*, Vol. 15, no. 2014, pp:1929-1958, 2014

[48]   K. Liu, G. Kang, N. Zhang and B. Hou, "Breast cancer classification based on fully-connected layer first convolutional neural networks,", *IEEE Access*, Vol. 6, pp:23722-23732, 2018

[49]   Y. LeCun, Y. Bengio, and G. Hinton, "Deep learning," *nature*, Vol. 521, no. 7553, pp:436-444, 2015

Article Information Form